Global particle simulations as a future model for Space Weather Program

Ken Nishikawa (Rutgers University)
Dong-Sheng Cai (University of Tsukuba)
Takashi Tanaka (Kyushu University)
Bertrand Lembege (CETP/UVSQ/IPSL)

The 27 EGS Meeting, April 21 - 25, 2002

Collaborators

Shin Ohtani (JHU/APL)	***Substorm observations***
Dong-Sheng Cai (Univ. Tsukuba)	***HPF code, Magnetic filed topology***
Bertrand Lembege (CETP/IPSL)	***Particle simulations, AVS, Cluster***
Takashi Tanaka (CRL)	***MHD simulations with TVD method***
Wendell Horton (UT Austin)	***Substorm theory***
Mike Schulz (Lockeed)	***Particle acceleration theory***
Shinobu Machida (Kyoto Univ.)	***Magnetotail observations***
Tom Moore (GSFC)	***Ionospheric outflows***
Shigeto Watanabe (Hokkaido Univ.)	***Ionospheric observations***
Jean-Andre Sauvaud (CESR/CNRS)	***Interball & Cluster Observations***
Tai Phan (UCB**)**	***Dayside reconnections***
Tsugunobu Nagai (Tokyo Inst. Tech)	***Bursty Bulk Flows***
Norman Zabusky (Rutgers University)	***3-D graphics* (*Visiometrics*)**
David Sibeck (JHU/APL)	***HFAs***
Ryuho Kataoka (Tohoku University)	***HFA Simulations***

Outline

- **Introduction**
  - **A brief history of global simulations**
  - **Comparisons among the different methods**
  - **Plasma parameters**
- **Motivations and Objectives**
- **Simulation with a southward turning IMF**
  - **Synergetic processes for substorm onset**
- **Summary**
- **Future work**

Various methods

- **MHD simulations (since 1981) provide a quantitative picture**

  without kinetic effects
- **Tailored simulations with modules**

  work well with local simulations, can be combined with MHD simulations
- **Hybrid simulations [*Quest and Karimabadi*, ISSS-6, 2001]**

  electrons fluids (Quest: it will be done in five years at ISSS-6)
- **Global particle simulation**

  difficult to establish good spatial and temporal resolutions with a reasonable mass ratio at the present time, but it will become a vital model
- **MHD simulations with localized particle simulations**

  very difficult to transfer physical values at boundaries

A brief history of global simulations

- **1978: First 2-D MHD simulations by Leboeuf et al.**
- **Early 80's: First 3-D MHD simulations (Brecht, Lyon, Wu, Ogino)**
- **Late 80's: Model refinements (FACs, ionosphere, higher resolution, fewer symmetries)**
- **Early 90's: Long geomagnetic tail, refined ionosphere models.**
- **1992: First global particle simulation (Buneman et al.)**
- **Mid 90's: ISTP is well under way, first comparisons with *in situ* space observations and ground based observations. Beginning of *quantitative modeling*.**
- **1997: First particle simulations with southward IMF (Nishikawa)**
- **Late 90's: Global modeling has become an integrated part of many experimental studies. Models provide an extension to spatially limited observations and help us to understand the physics**
- **1998: First particle simulation with dawnward IMF confirmed with MHD simulations (Nishikawa) (MHD: White et al., 1998)**
- **2000: Large-scale kinetic (LSK) model for the origin of the near-Earth plasma population during a substrom (Ashour-Abdalla et al.)**
- **2001: A substorm model by global particle simulation (Nishikawa)**

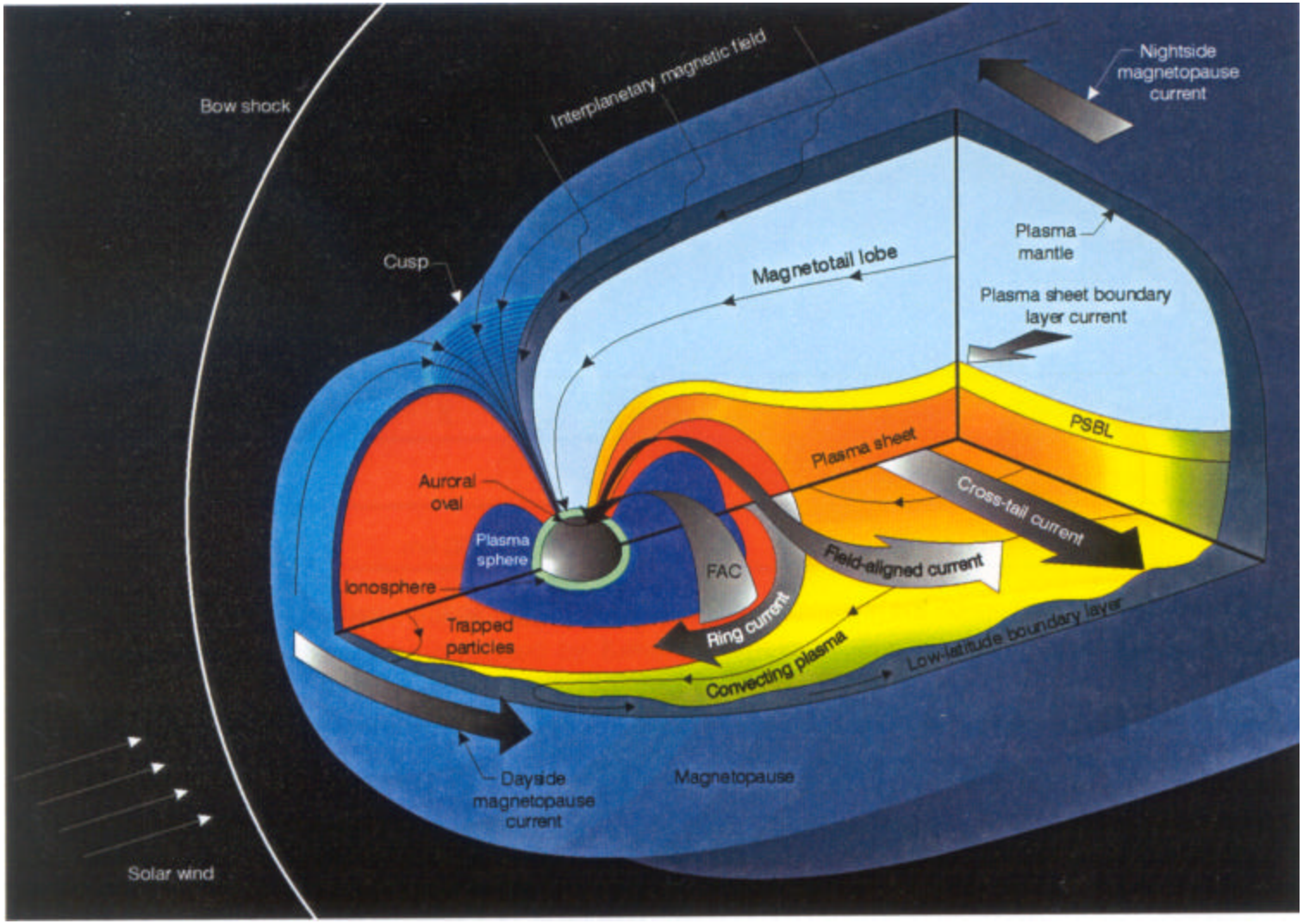

What triggers a substorm?

How are high energy particles injected during substorms and storms?

How is a ring current generated and dissipated with ionospheric outflows particles (storm-substorm relationship)?

Present global particle simulations can do

Reproduce the gross features of Magnetosphere including

a reasonable (qualitative) representation of

- **the bow shock**
- **the magnetopause**
- **the cusps**
- **the magnetotail**
- **the effects of the IMFs (reconnections, particle injections)**
- **fields and currents**

Reproduce the fundamental features of the dynamic Magnetosphere:

- **substorms**
- **transient events due to variations of solar wind conditions**
- **convections**
- **particle acceleration**

MHD simulations with kinetic aspects at the present time

- **Embedding small-scale algorisms in MHD simulations:**

  anomalous resistivity, microscopic effects,

  using a generalized Ohm's law ($E = -v \times B + \eta J + (J \times B - \nabla p_e)/qn$)

  Hall term: including the ion kinetic effects at the ion inertial length

- **Trace particles (ions and electrons) (not self-consistent) using the electromagnetic fields obtained by MHD simulations [***Walker et al., Space Sci. Rev., 88, 1-2, 285, 1999***; *Walker et al., AGU Monog, accepted, 2001*]**

- **Combining with other modules:**

  RCM, Ionospheric models, local particle (hybrid) simulations

- **Hybrid simulations: (the scale of electron Debye length is not included)**

  Fluid electron (save memory) [*Quest and Karimabadi*, ISSS-6, 2001]

Particle tracing with MHD simulation (ions)

Walker et al., Modeling Magnetospheric Sources, AGU Monog., in press, 2001

Southward IMF

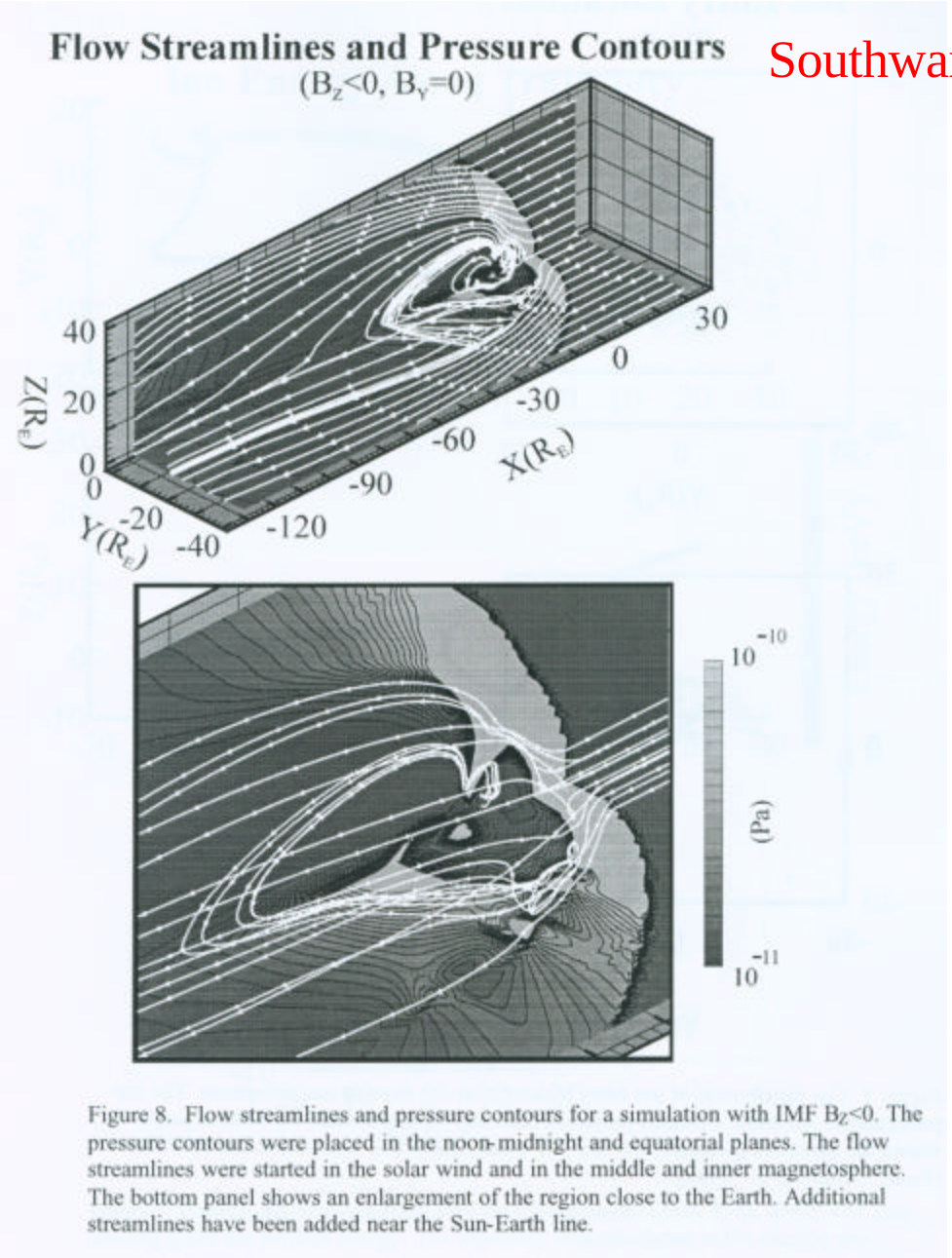

Figure 8. Flow streamlines and pressure contours for a simulation with IMF B_Z<0. The pressure contours were placed in the noon-midnight and equatorial planes. The flow streamlines were started in the solar wind and in the middle and inner magnetosphere. The bottom panel shows an enlargement of the region close to the Earth. Additional streamlines have been added near the Sun-Earth line.

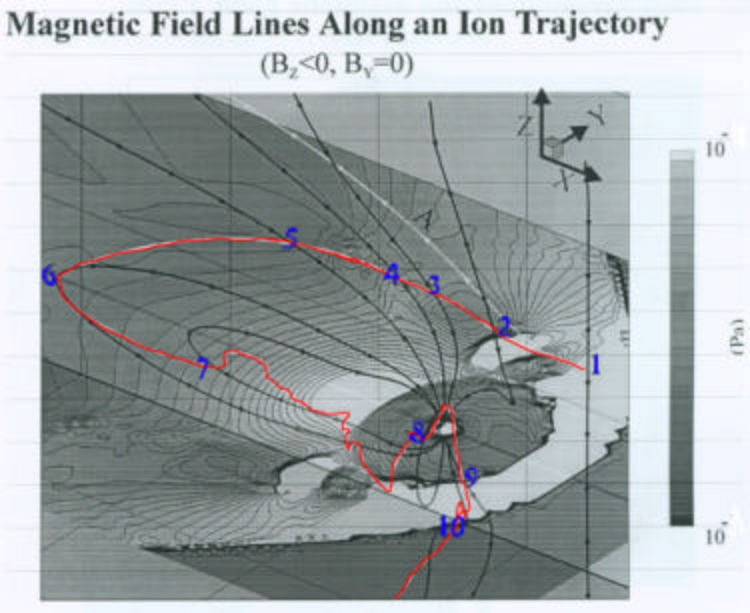

***Similar research* (*LSK model*)**

Ashour-Abdalla et al., The origin of the near-Earth plasma population during a substorm on November 24, 1996, JGR, 105, 2589, 2000.

Ions observed at Geotail are traced back.

Particle injections into the tail with southward IMF

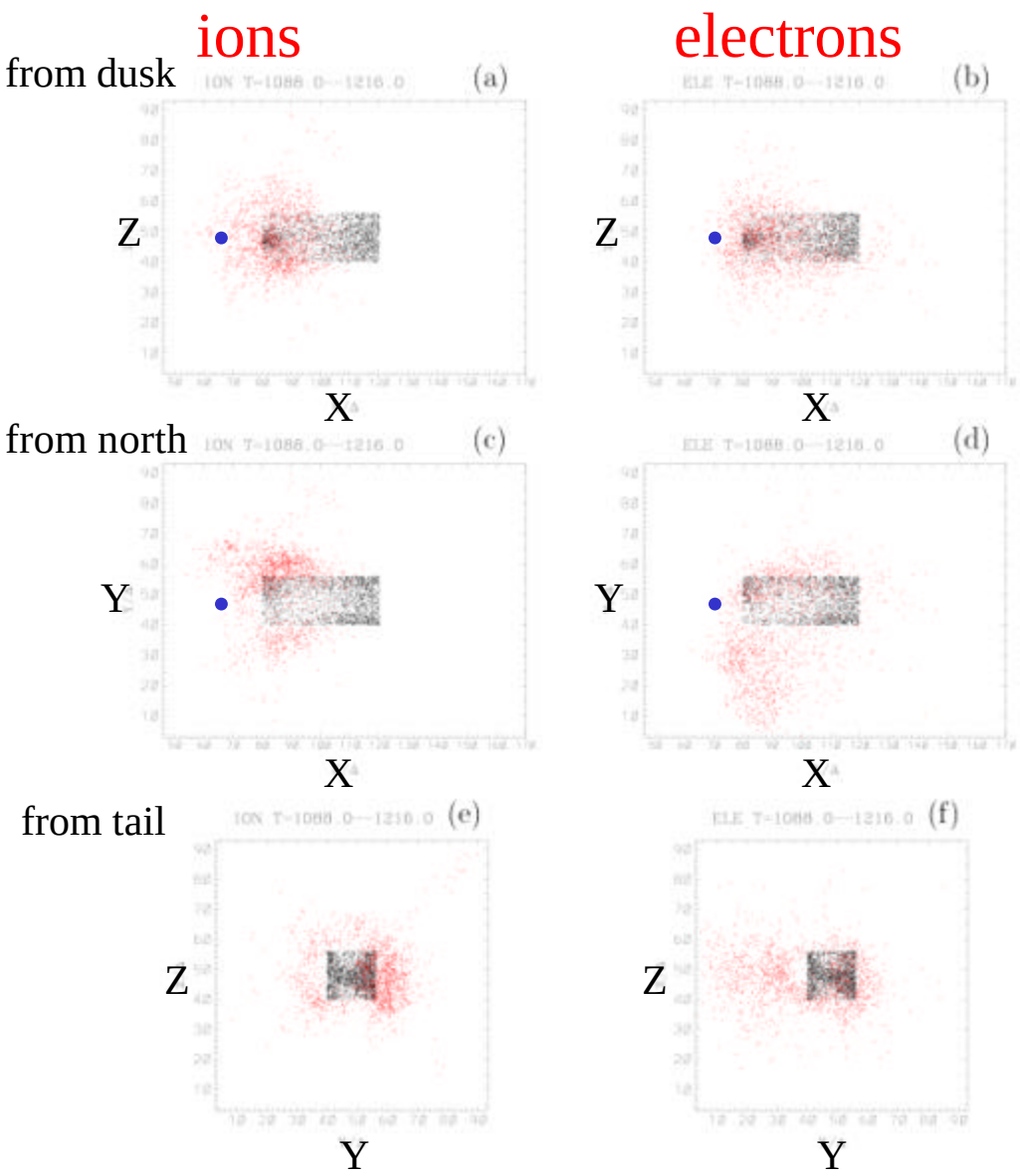

- at 0.10UT (before subsorm)
- at 0.30UT (later)

near-Earth tail box-shaped region

$-10R_E \geq x \geq -40R_E$

$8R_E \geq y, z \geq -8R_E$

Ions: from dawnside

Electrons: from duskside

- Earth

(Nishikawa, JGR, 1997)

Comments on our global particle simulations

Peroomian, Ashour-Abdalla, & Zelenyi, JGR, 105, 18,807, 2000

"To address this issue (Consistent orbit tracing (COT)), Nishikawa [1997,1998a,b] and Nishikawa and Ohtani [1998] models the magnetosphere using full three-dimensional (3-D) global kinetic simulations. These simulations have resulted in a ***better understanding of the interaction of the solar wind with the magnetosphere and yielded a self-consistent picture of the nightside magnetic field***. However, the ion to electron mass ratio in their simulations was 16, and the grid size was of order of $1\boldsymbol{R}_E$, approximately equal to the Debye length. Thus only extremely coarse details of resulting solution could be discerned. Given today's computing capacities, it is necessary to compromise on the grid size and mass ratio to globalize full kinetic models of entire magnetosphere. **These limitations will be of course be reduced with the development of increasingly sophisticated computer techniques**."

Local vs. global simulations of magnetotail reconnections

	local	global
resolutions	0.1 - 0.01$\boldsymbol{R}_E$	1 - 0.4$\boldsymbol{R}_E$
dawn-dusk BC	none (periodic)	yes (self-consistent)
Earth side BC	not realistic (at 5-6$\boldsymbol{R}_E$)	self-consistent
shape of Earth	cylinder	sphere
effects of IMFs	imposing $\mathbf{E}_y$ externally	self-consistent
study of physics	attainable	difficult
initial conditions	not easy	self-consistent
dayside effects	not included	self-consistent
ionosphere	not included	partially included

Why do we need to use particle simulations?

*** In MHD simulations some of kinetic effects are not included**

- **dynamics of boundaries are not properly simulated**
- **particle injections are not included in MHD simulations,**
  in particular accelerated high energy particles
- **ring current is not included in MHD models at the present time**

*** Computer power (memory and speed) will be available in**
ten years or so in order to perform global particle simulations for
quantitative comparisons with observations including velocity distributions

*** Prepare for future missions such as MMS (2006) and MC DRACO (2010)**
in order to provide useful information for planning and data analysis

*** Predictions of high energy particle injections for Space Weather Program**

Complementary with MMS

- **Single spacecraft have only glimpsed micro- and macro-physical processes.**
- **The next logical step is to deploy spacecraft "networks" and requires both:**
- **<u>MMS</u> to resolve smaller size and shorter time scales; and,**
- **<u>DRACO</u> to resolve larger size and longer time scales.**

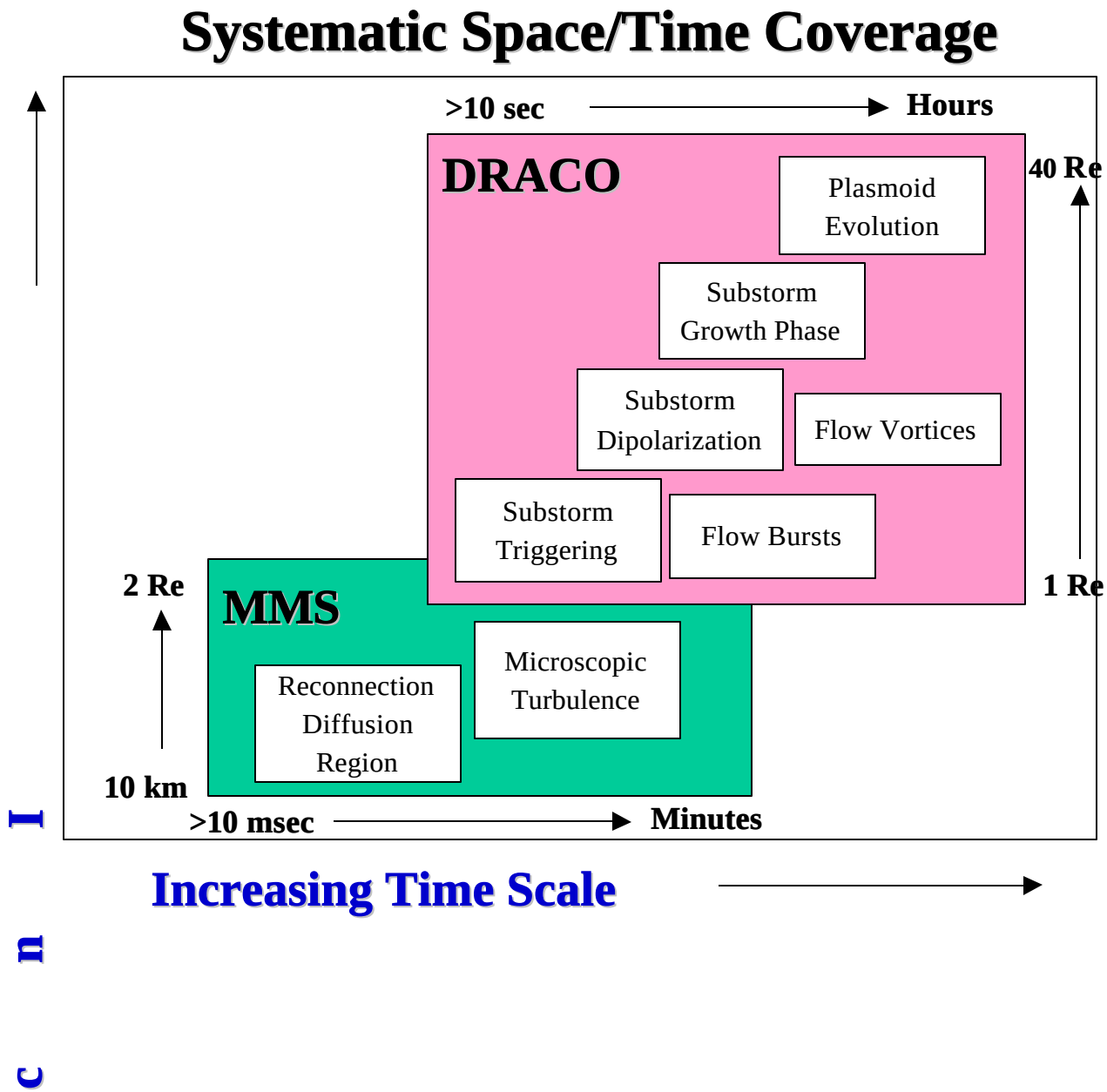

Basic equations

Maxwell equations

$$\partial \boldsymbol{B}/\partial t = -\nabla\times\boldsymbol{E} \quad \text{and} \quad \partial \boldsymbol{D}/\partial t = \nabla\times\boldsymbol{H} - \boldsymbol{J}$$

As well as Newton-Lorentz (relativistic)

$$d m\boldsymbol{v}/d t = q(\boldsymbol{E} + \boldsymbol{v}\times\boldsymbol{B})$$

$$\varepsilon_0 = 1 \quad \text{and hence} \quad \mu_0 = 1/c^2$$

$$\boldsymbol{D} = \boldsymbol{E} \quad \text{and} \quad \boldsymbol{B} \rightarrow c\boldsymbol{B}$$

$$\boldsymbol{E} \Leftrightarrow \boldsymbol{B} \quad \text{(symmetric)}$$

Plasma parameters

$\omega_e = (nq_e^2/m_e)^{1/2}$: electron plasma frequency

$\omega_i = (nq_i^2/m_i)^{1/2}$: ion plasma frequency

$\Omega_e = q_eB/m_e$: electron gyrofrequency

$\Omega_i = q_iB/m_i$: ion gyrofrequency

$\lambda_e = v_e/\omega_e$: electron Debye length (***ignored in Hybrid simulations***)

$\lambda_i = v_i/\omega_i$: ion Debye length

$\lambda_{ce} = c/\omega_e$: electron inertial length

$\lambda_{ci} = c/\omega_i$: ion inertial length

$\Delta x \geq 3\lambda_e$: (to avoid numerical instability)

$\Delta t \leq \Delta x/c$: Courant (CFL) condition (c = 0.5)

if $c = 10v_e$, $T_i = T_e$, and m_i/m_e=**16**	if $c = 20v_e$, $T_i = T_e$, and m_i/m_e=**100**
$\lambda_e << \lambda_i << \lambda_{ce} << \lambda_{ci}$	$\lambda_e << \lambda_i << \lambda_{ce} << \lambda_{ci}$
1 4 10 40	1 10 20 200

Numerical considerations

- **Scale Size**
  - ➤ **the scale of the system ranges from 10s of Kms in the ionosphere to 100s of Earth radii in the far tail. Þ unstructured grids**
  - ➤ **physical values vary up to 7 orders of magnitude, e.g.,**

    $B \sim (10^{-2} – 10^{4})$nT, $\beta \sim (10^{-5} – 10^{2})$, $n \sim (10^{-2} – 10)/cm^3$
- **Time step**
  - ➤ **the smallest time step is considered by the fastest wave speed in the system, which is of order of the fast mode speed – this can be very high near the Earth.**
- **Verification**
  - ➤ **one of the best tests of a numerical method is to compare its results with observations – however, since the observations are usually single or dual, the comparisons are not easy or comprehensive. (Establish a scaling law)**

Prospective improvements on simulation parameters

1990 – 1992: 105 ´ 55 ´ 55 grids, 0.4 M particles (1/cell) (45MB)

1992 – 1997: 215 ´ 95 ´ 95 grids, 4 M particles (1/cell) (0.3GB)

1998 – 2001: 85 ´ 105 ´ 105 grids, 6.4 M particles (4/cell) (0.5GB)

2001 – 2002: 500 ´ 250 ´ 250 grids, 600 M particles (10/cell) (30GB)

2002 – 2003: 1000 ´ 500 ´ 500 grids, 600 G particles (100/cell) (300TB)

TSC1 at PSC: 2.7 TB, Earth Simulator: 300TB (2002)

2010 – 2012: 10000 ´ 5000 ´ 5000 grids, 50 T particles (100/cell) (2400TB)

Distributed Terascale Facility (DTF): 650 terabytes, TeraGrid

Year	1999	2001	2003	2005	-	2010
Grid size	$1R_E$	$0.4R_E$	$0.2R_E$	$0.1R_E$	-	$0.005R_E$
Mass ratio	16	16	25	36	-	100

M:10^6 G:10^9 T:10^{12}

Postprocessing

- **Snapshots (NCARG, Techplot, AVS)**
  - **electron (ion) density at any cross-sections**
    - **with arrows (magnetic fields, fluxes)**
  - **electron (ion) flux (velocity) with arrows**
    - **(flux (velocity) in the cross-section)**
  - **3-D displays of isosurface**
  - **streamlines of magnetic fields (velocity)**
- **Time-dependent**
  - **movies (electron density, magnetic field lines, etc)**
  - **local electromagnetic fields (E, B)**
  - **sheet currents in the tail**
- **Requires new graphics depend on physics you would like to understand including virtual 3-D displays**

References of global particle simulations

1. **"Solar wind-magnetosphere interaction as simulated by a 3D EM particle code," Buneman, O., T. Neubert and K.-I. Nishikawa,** *IEEE Trans. Plasma Sci., 20*, **810, 1992.**
2. **"Solar wind-magnetosphere interaction as simulated by a 3D EM particle code," Buneman, O., K.-I. Nishikawa, and T. Neubert, in** *Space Plasmas: Coupling Between Small and Medium Scale Processes, Geophys. Monogr. Ser.,* **vol. 86, edited by M. Ashour-Abdalla, T. Chang, and P. Dusenbery, p. 347, AGU, Washington D.C., 1995.**
3. **"Particle entry into the magnetosphere with a southward IMF as simulated by a 3-D EM particle code," Nishikawa, K.-I.,** *J. Geophys. Res., 102*, **17,631, 1997.**
4. **"Reconnections at near-Earth magnetotail and substorms studied by a 3-D EM particle code," Nishikawa, K.-I.,** *Geospace Mass and Energy Flow: Results From the International Solar-Terrestrial Physics Program, Geophys. Monogr. Ser.,* **vol. 104, edited by J. L. Horwitz, W. K. Peterson, and D. L. Gallagher, p. 175, AGU, Washington D.C., 1998.**

5. **"Particle entry through reconnection grooves in the magnetopause with a dawnward IMF as simulated by a 3-D EM particle code," Nishikawa, K.-I.,** *Geophys. Res. Lett., 25*, **1609, 1998; MHD simulations [*White et al.*,** *GRL*, **1998]**

6. **"Evolution of thin current sheet with a southward IMF studied by a 3-D EM particle code," Nishikawa, K.-I. And S. Ohtani,** *J. Geophys. Res., 105*, **13,017, 2000.**

7. **"Global Particle Simulation for a Space Weather Model: Present and Future," Nishikawa, K.-I. And S. Ohtani,** *IEEE Trans. Plasma Sci., 28*, **1991, 2000.**

8, **"Global particle simulation study of substorm onset and particle acceleration," Nishikawa, K.-I.,** *Space Sci. Rev., 95*, **361, 2001.**

9. **"Visualization and criticality of three-dimensional magnetic field topology in the magnetotail," Cai, D.-S., Y. Li, T. Ichikawa, C. Xiao, and K.-I. Nishikawa,** *Earth Planets Space*, **53, 1011, 2001.**

Motivations for global particle simulations

- **Kinetic processes reveal essential physics involved in substorms and storms**
- **Investigate energetic particle injections into inner magnetosphere and ionosphere originated from the solar wind particles**
- **Contribute to new NASA missions such as Cluster II (ESA), Magnetospheric Multiscale Mission and Magnetospheric Constellation that provide data with microscopic processes (velocity distributions) with future significant improvements in simulation and physical parameters**
- **3-D Electromagnetic Particle Model (EMPM) for Space Weather Program is a challenging project, however it is necessary for predicting high energy particle injections**
- **Take advantage of modern supercomputers using parallel processing (HPF) on ORIGIN2000**

Objectives

- **What is the time sequence of tail dynamics with southward turning IMF?**
- **When does the reconnection take place?**
- **How are earthward flows (BBFs) generated?**
- **What is the relationship among reconnection, BBFs, flow braking, and CD?**
- **When and how does the dipolarization occur?**
- **What is the main mechanism of substorm triggering?**
- **How does the IMF B_y component affect these processes?**
- **How is the ring current generated with storms?**
- **How is the ring current generation affected with prior substorms?**
- **How are energetic particles generated and how are they injected into the inner magnetosphere?**

Coupling between magnetotail regions

(One of *MC DRACO's scientific objects*)

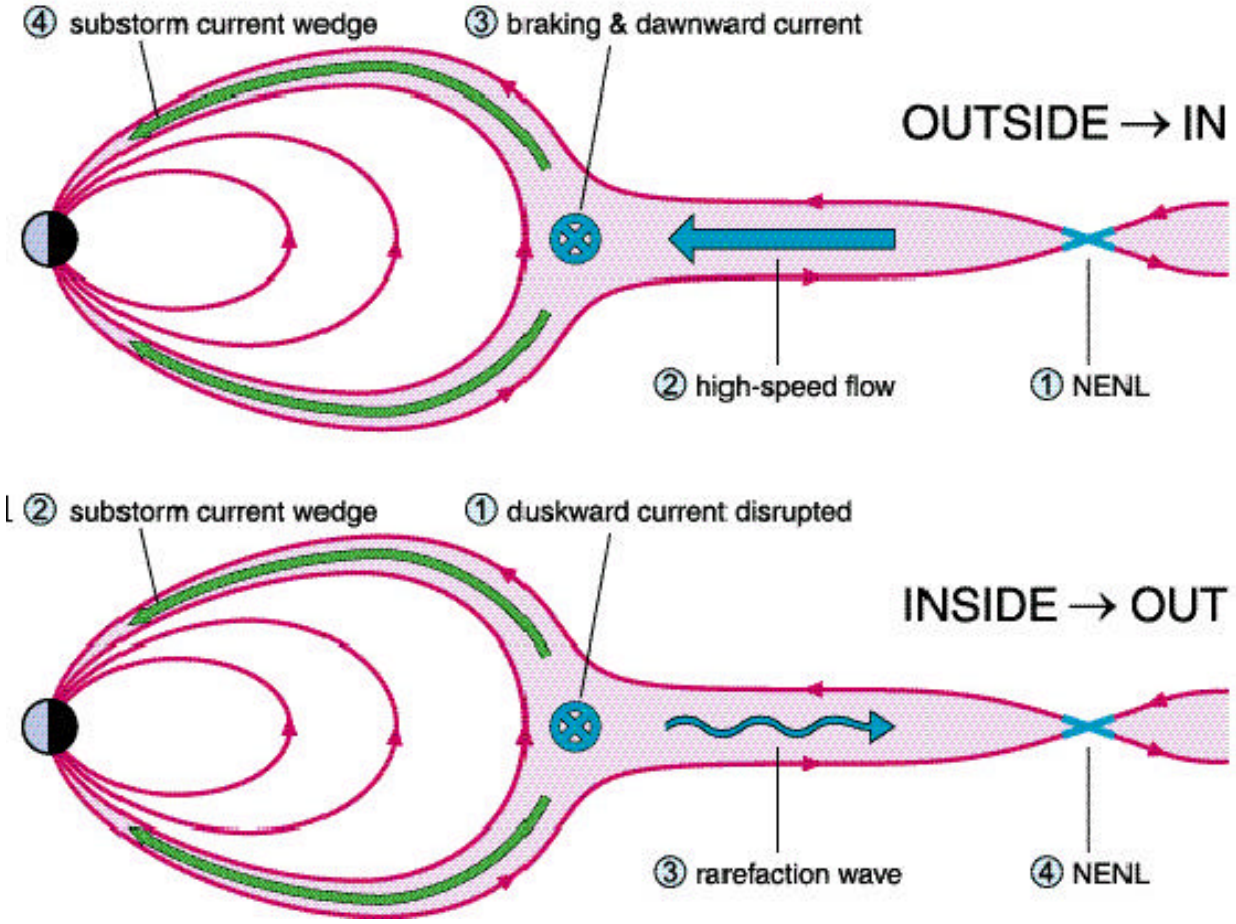

[*Lui*, SSR, 95, 325, 2001]

Tail observations

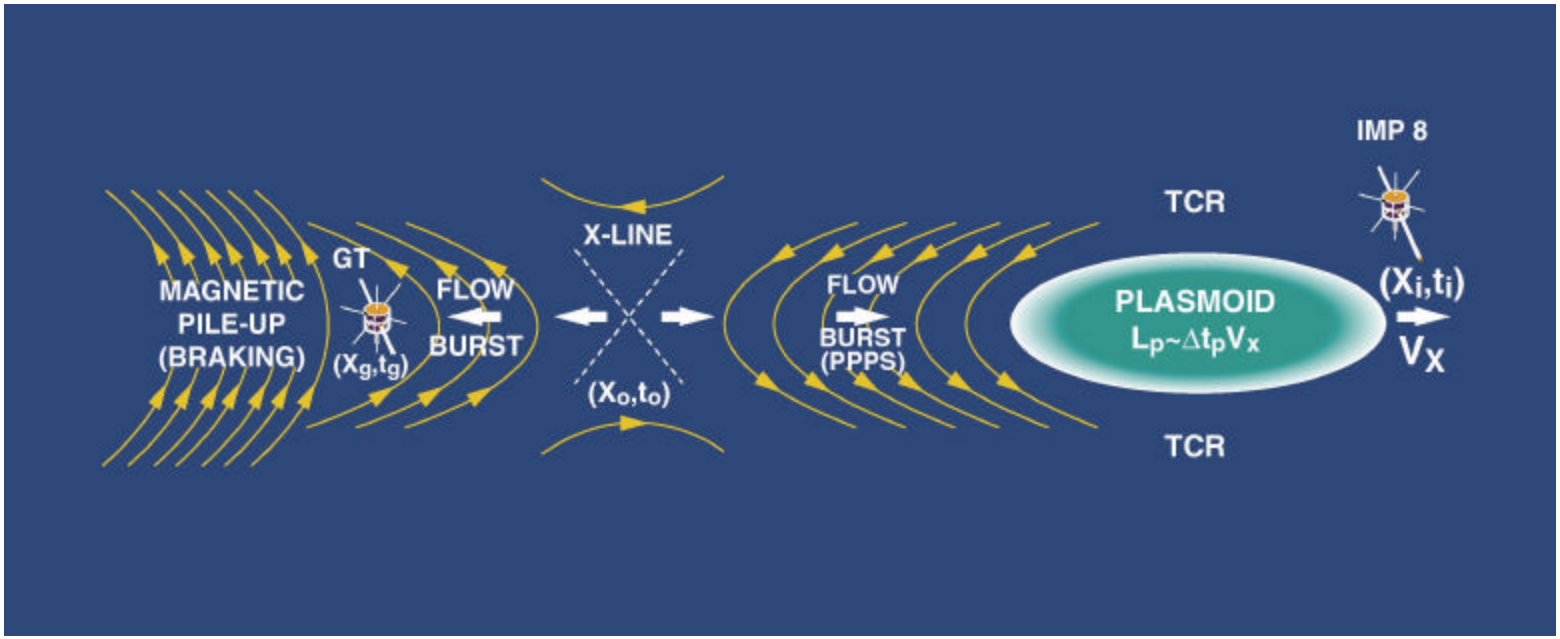

Figure 11 Meridian cut through the central tail showing the earthward and tailward consequences of onset of open field line **reconnection**; earthward and tailward high-speed flows, flow braking and dipolarization, plasmoid ejection from [*Slavin et al*. JGR, submitted, 2000]

Multi-satellite observations (Ohtani et al. JGR, 104, 22,713, 1999)

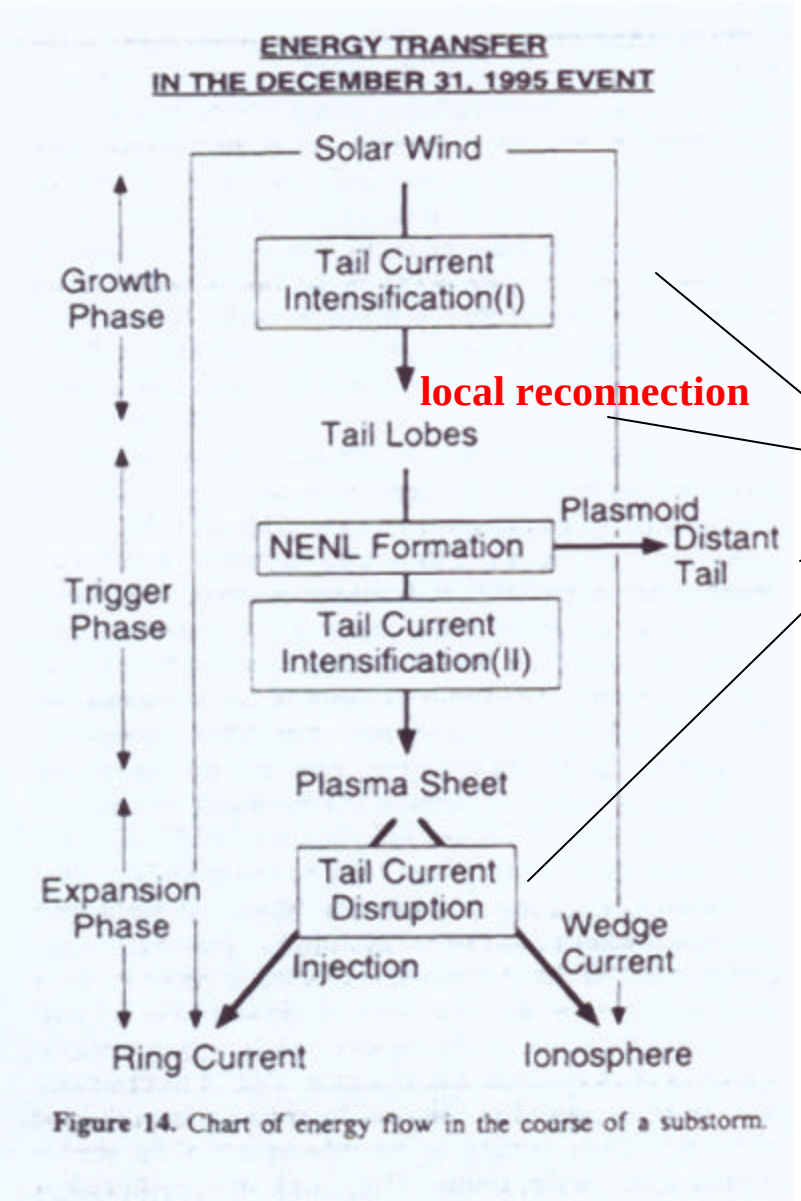

Figure 14. Chart of energy flow in the course of a substorm.

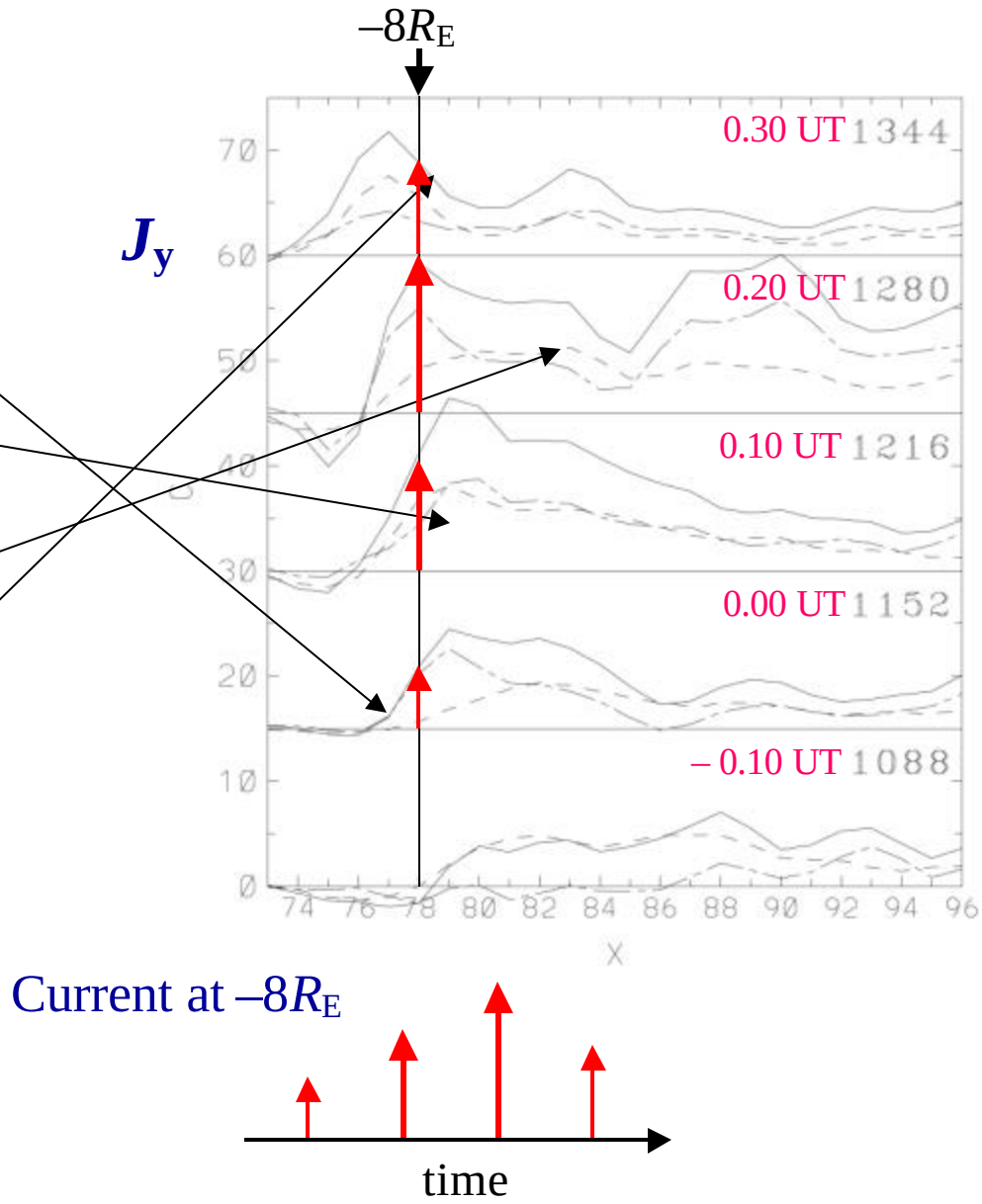

Summary of simulations

Solar wind with southward IMF

ß

Sheet current becomes maximum
(Local reconnections occur)

ß

***Full* Reconnection takes place**

ß ß

Peak of sheet current moves Earthward | **Earthward flows are generated**

ß ß

Current disruption | **Flows brake**

ß ß

Dipolarization | **Dawnward current**

ß Û ß

Wedge Current is generated?

Magnetic field lines in 2-D (noon-midnight)

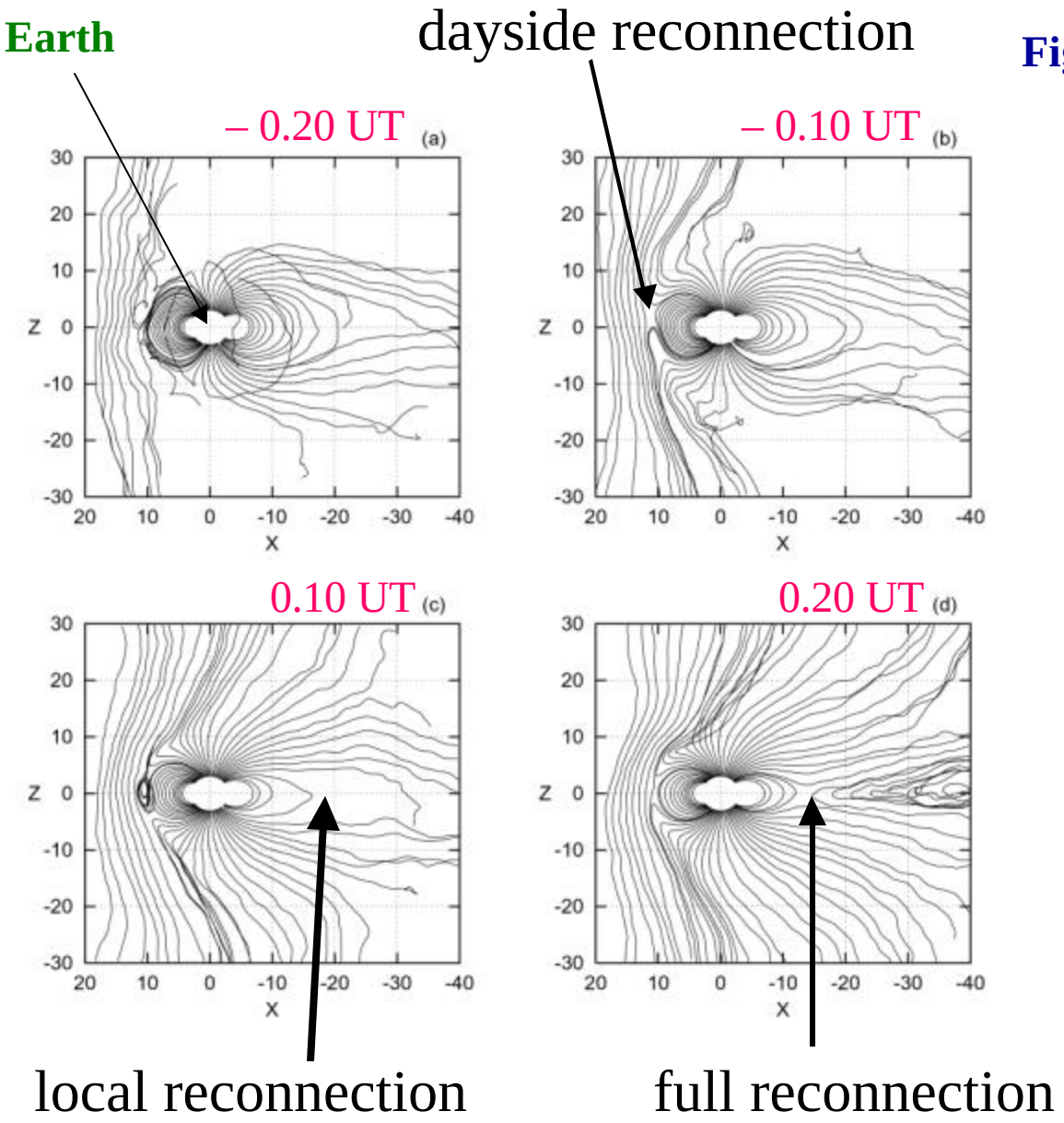

Figure 1 shows the magnetic field lines in the noon-midnight meridian plane (GSM) containing the dipole center at step (a) – 0.20 UT (1024), (b) – 0.10 UT (1088), (c) 0.10 UT (1216), and (d) 0.20 UT (1280). The magnetic field lines are traced from near the Earth ($r = 3\Delta$, ($\approx 3R_E$)) and subsolar line in the dayside and the magnetotail. Some magnetic field lines are moved dawnward or duskward. The tracing was terminated due to the preset number of points or the minimum strength of total magnetic field.

Changes from the marginal state to reconnection

[*Cai et al.*, *Earth Planet Space*, 53, 1011, 2001]

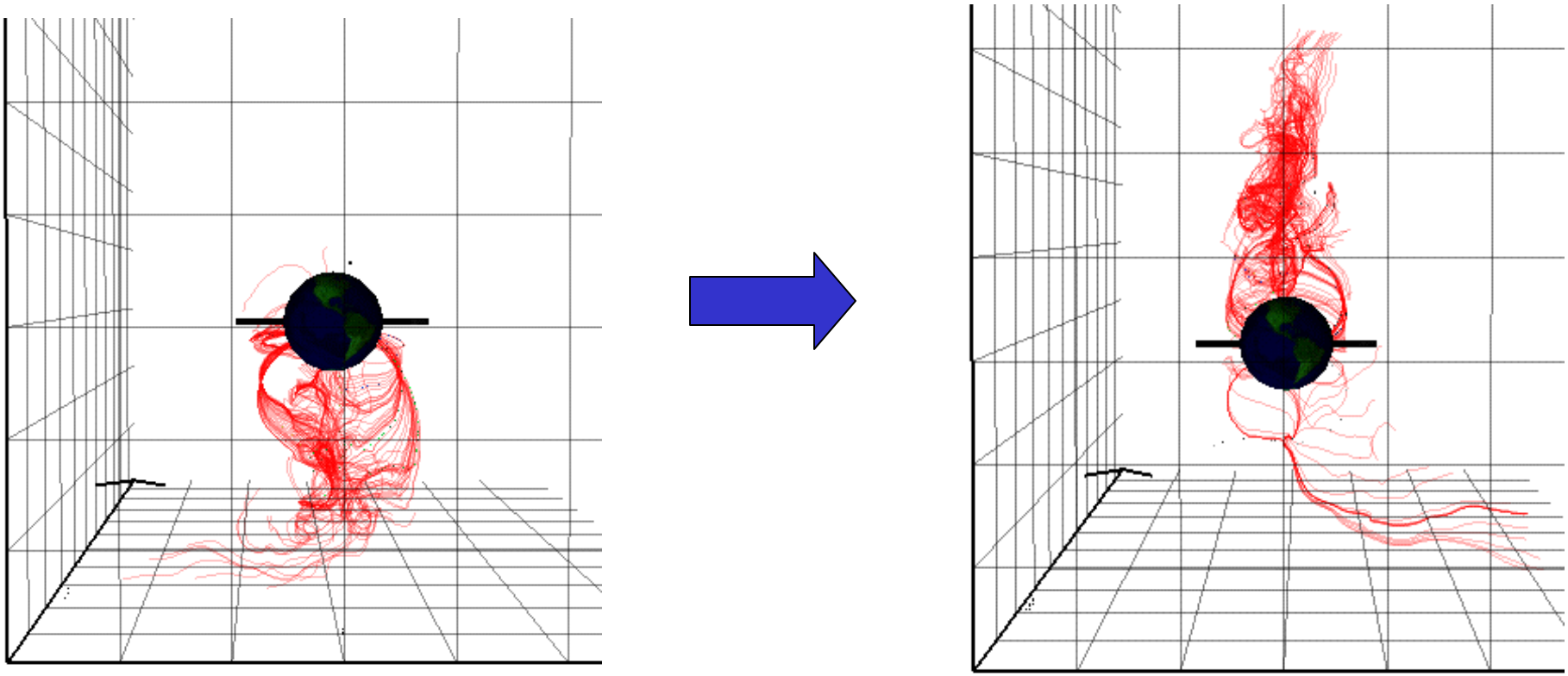

Averaged current density J_y (× 10) along the subsolar line

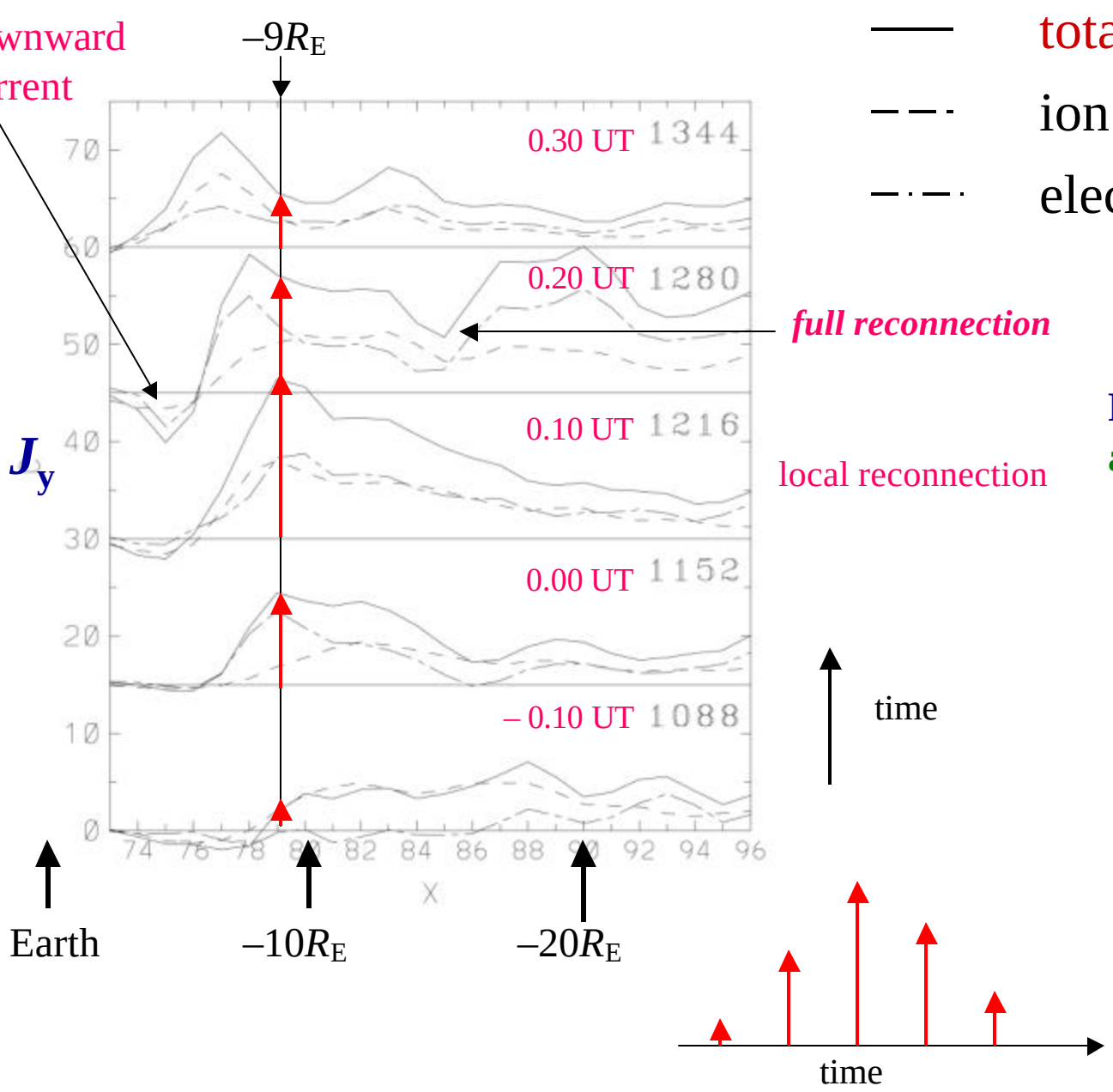

Figure 2 shows the **averaged current density** J_y in the noon-midnight meridian cross section at time – 0.10 UT (1088), 0.00 UT (1152), 0.10 UT (1216), 0.20 UT (1280), and 0.30 UT (1344) [*Nishikawa and Ohtani*, 2000a].

ion flux 0.20 UT velocity in the x – z plane **viewed from the tail**

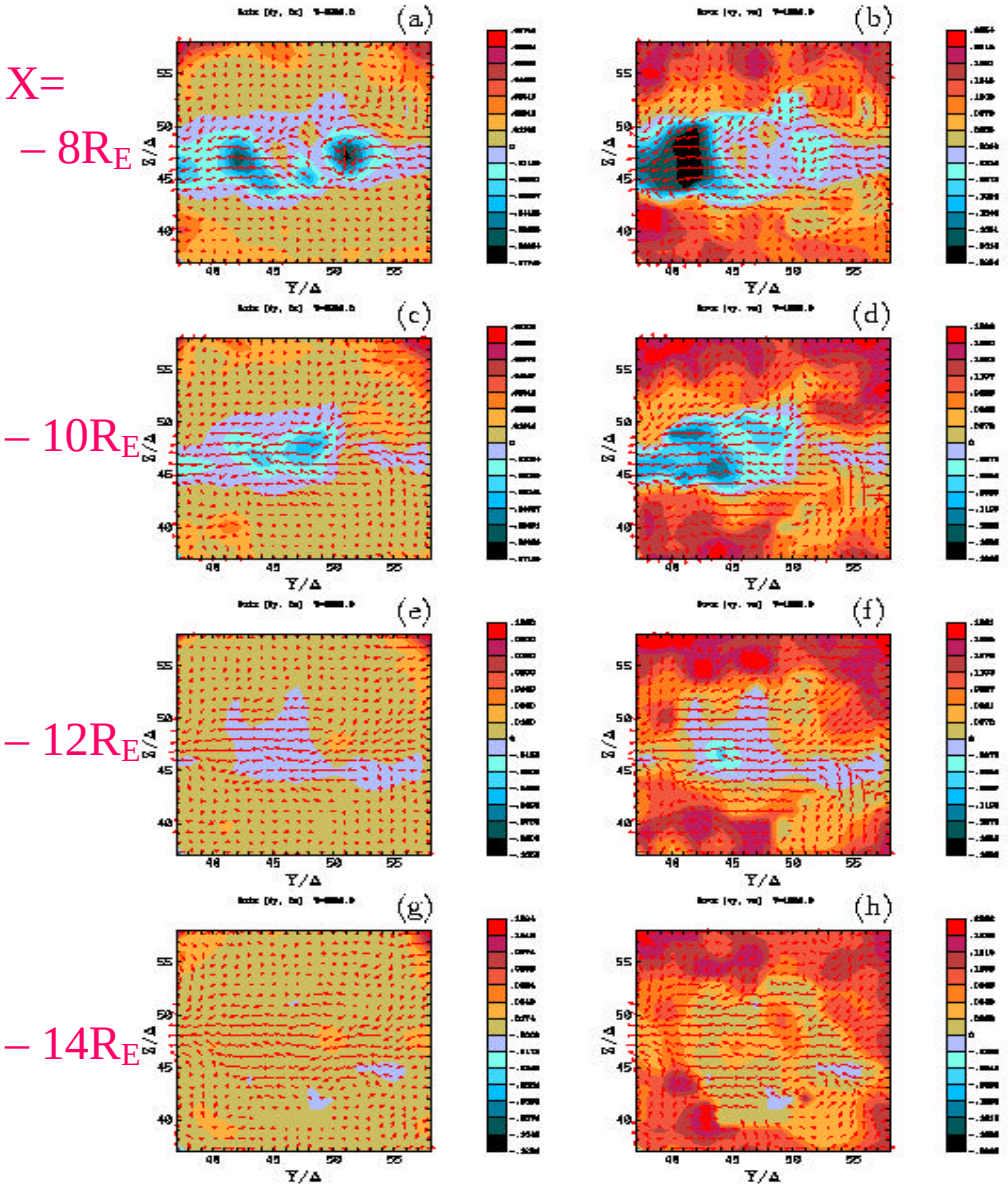

blues: earthward

reds: tailward

arrows: (V_y, V_z)

Figure 3 shows the ion flux (a, c, e, and g) and velocity (b, d, f, and h) in the dusk-dawn cross section plane at $x = -8\ R_E$ (a and b), $-10\ R_E$ (c and d), $-12\ R_E$ (e and f), $-14\ R_E$ (g and h) at time 0.20 UT (1280).

electron flux 0.20 UT velocity in the x – z plane **viewed from the tail**

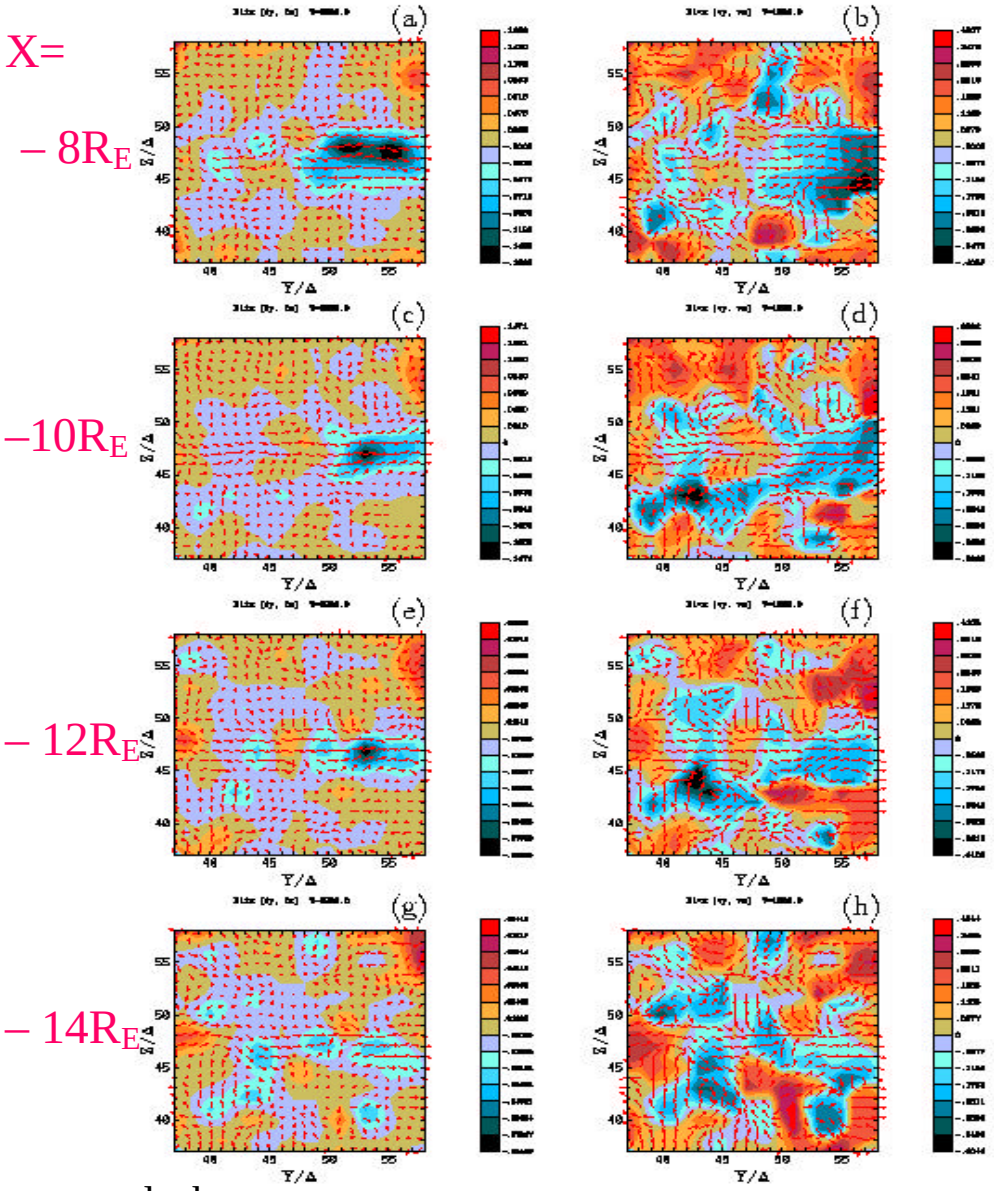

blues: earthward

reds: tailward

arrows: (V_y, V_z)

Figure 4 shows the electron flux (a, c, e, and g) and velocity (b, d, f, and h) in the dusk-dawn cross section plane at x = –8 R_E (a and b), –10 R_E (c and d), –12 R_E (e and f), –14 R_E (g and h) at time 0.20 UT (1280).

ion velocity electron dusk-dawn plane at x = –10 R_E

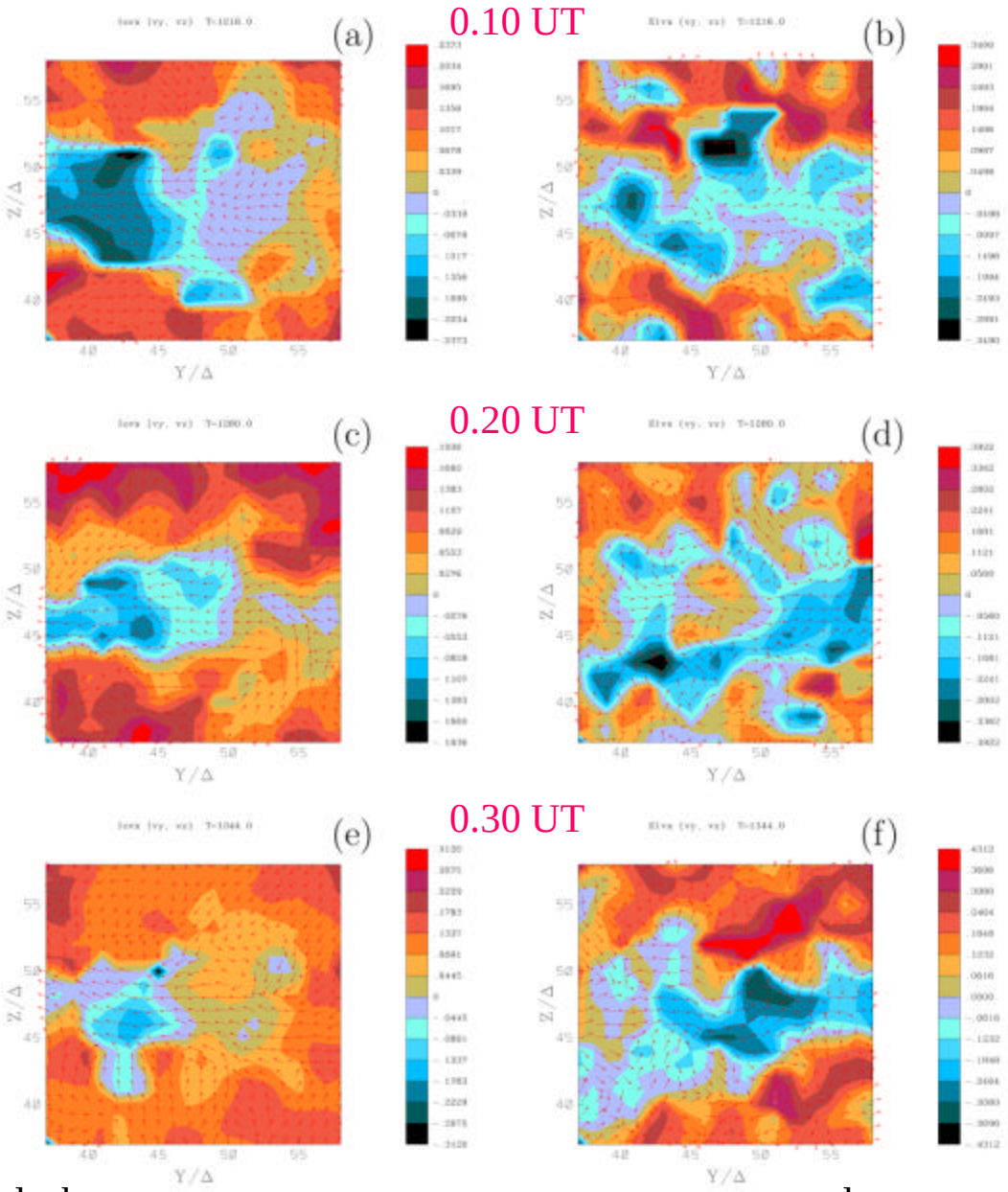

blues: earthward

reds: tailward

arrows: (V_y, V_z)

Figure 5 shows evolution of ion (a, c, and e) and electron (b, d, and f) velocities on the dusk-dawn cross section plane at x = 80Δ at time (a and b) 0.10 UT (1216), (c and d) 0.20 UT (1280), and (e and f) 0.30 UT (1344). The arrows show the ion (a, c, and e) and electron (b, d, and f) velocities on the plane (rescaled to show small values).

ion electron ***flow braking*** at the equatorial plane

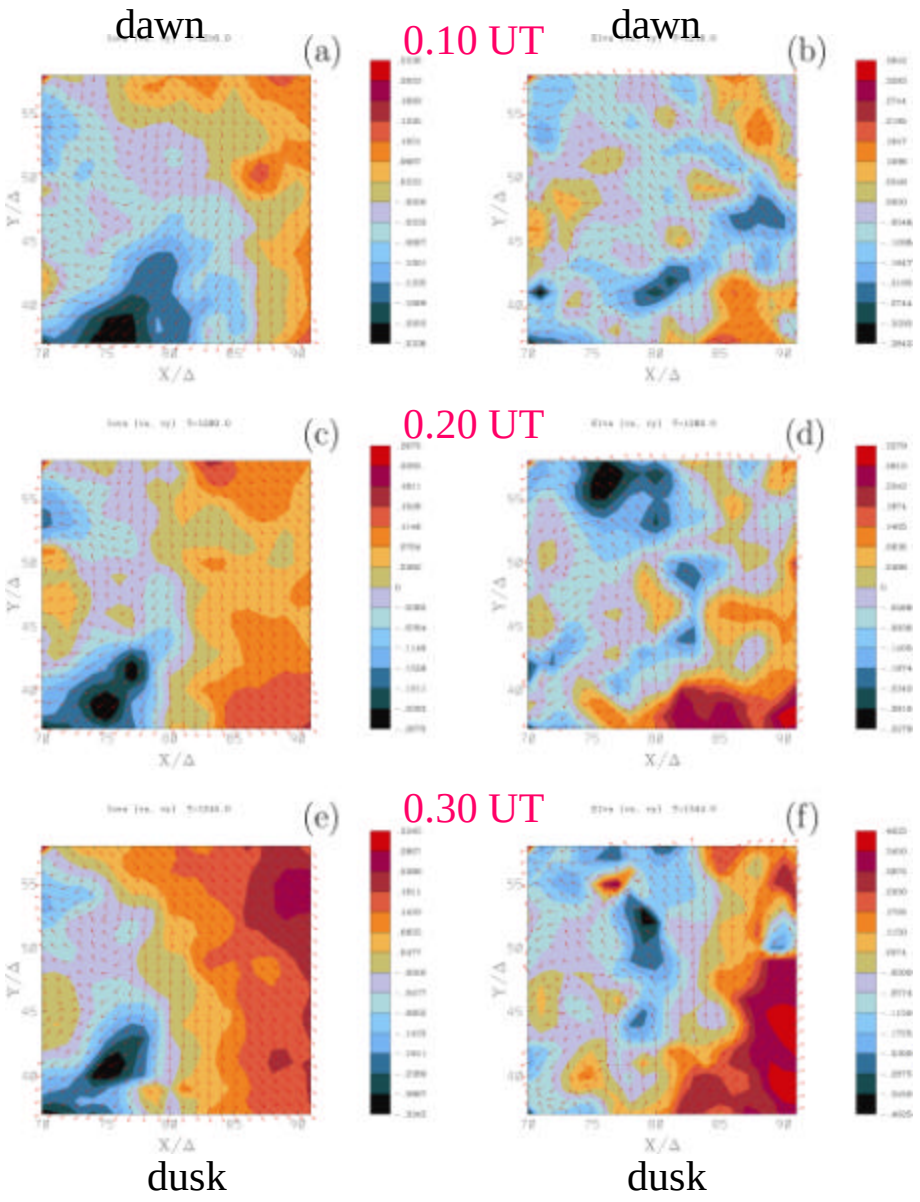

Figure 6 shows evolution of ion (a, c, and e) and electron (b, d, and f) velocities in the equatorial plane at z = 48Δ at time (a and b) 0.10 UT (1216), (c and d) 0.20 UT (1280), and (e and f) 0.30 UT (1344). The arrows show the ion (a, c, and e) and electron (b, d, and f) velocities on the plane (rescaled to show small values).

arrows: (V_x, V_y)

Ions → duskward

Electrons → dawnward

tailward

earthward

Earth

Comparison with observations

0.30 UT

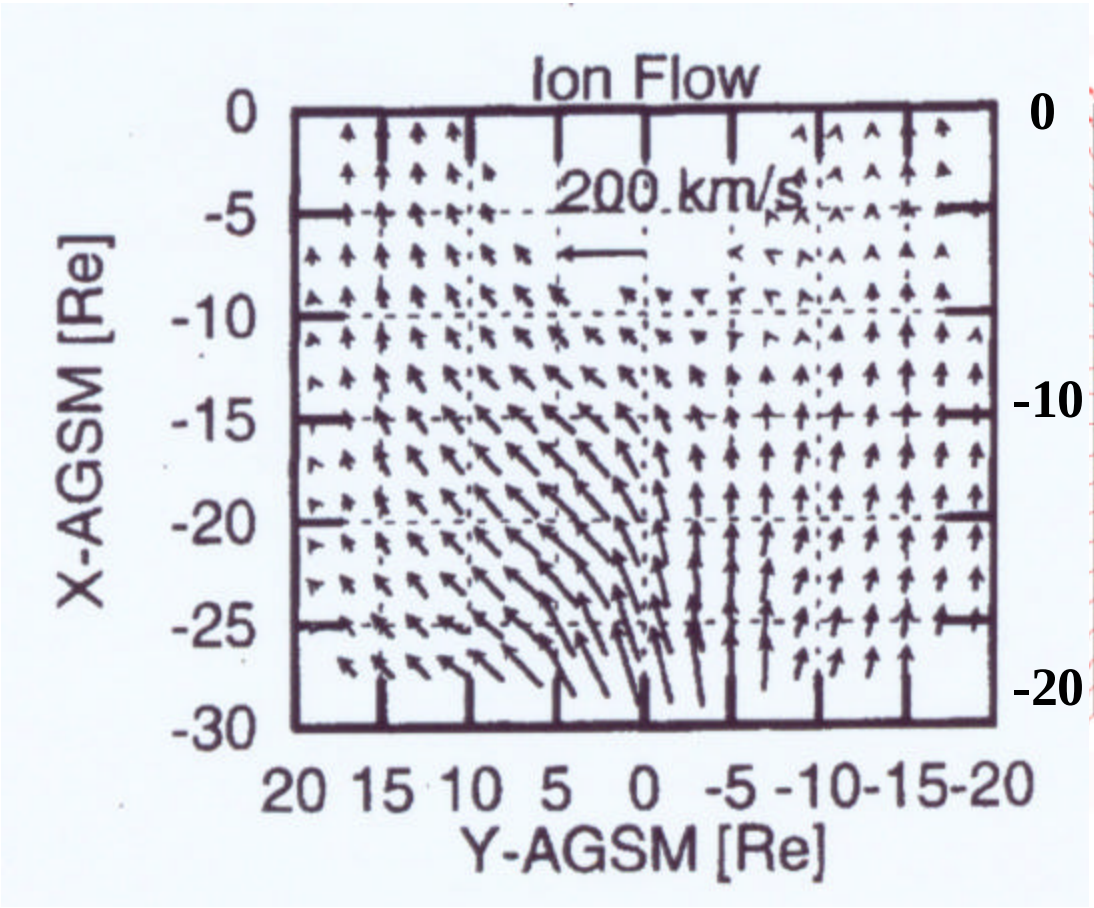

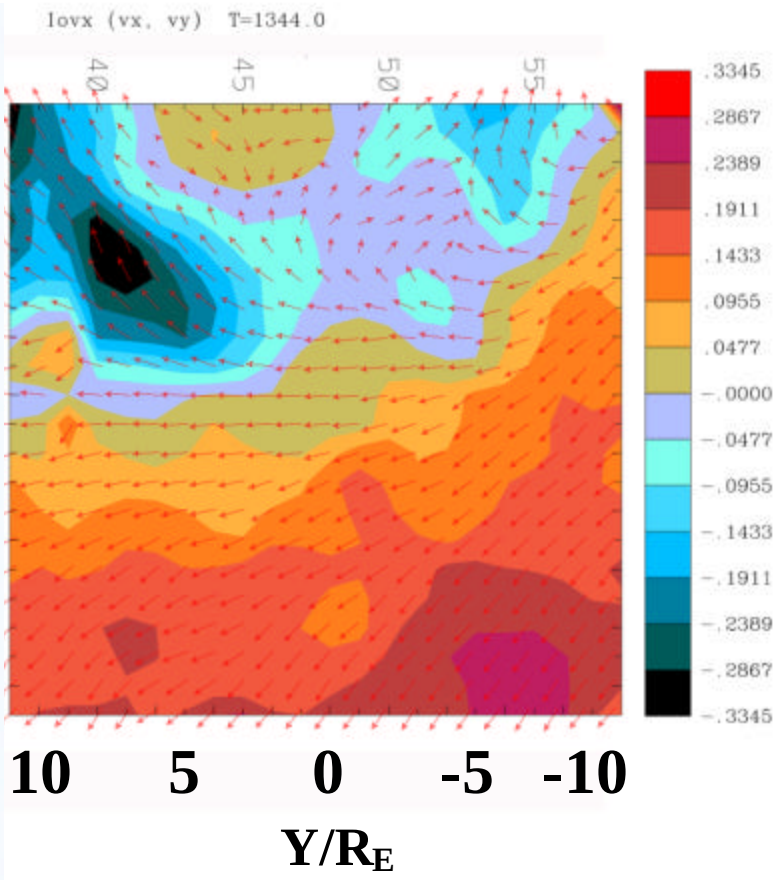

Averaged ion flow pattern in the plasma sheet (Geotail observations)

Earth

Diploarization seen in the noon-midnight meridian plane

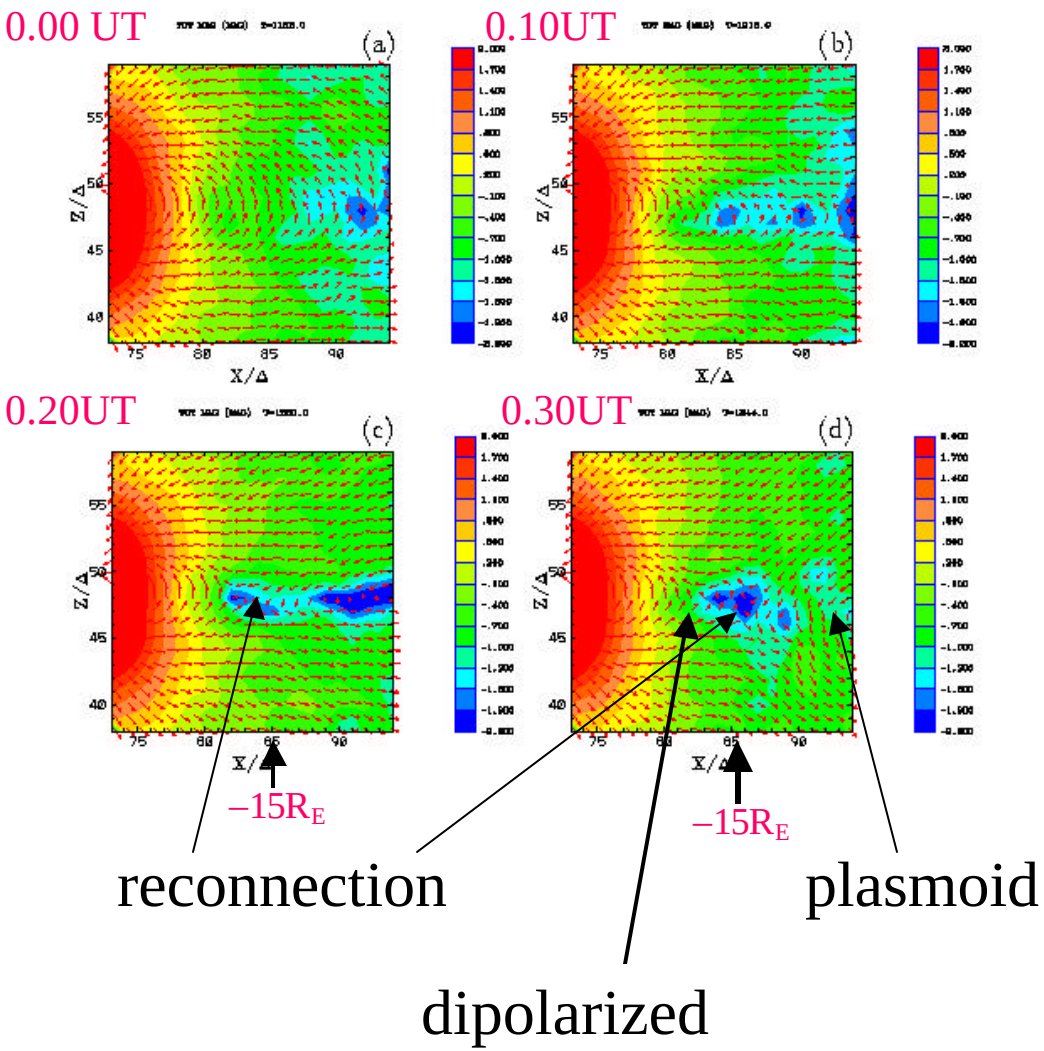

colors: log $|\boldsymbol{B}_{tot}|$

arrows: (B_x, B_z)

Figure 7 shows the ***total magnetic field*** strength in the noon-midnight meridian cross section (x – z) plane in the near-Earth magnetotail at time (a) 0.00 UT (1152), (b) 0.10 UT (1216), (c) 0.20 UT (1280), and (d) 0.30 UT (1344). The arrows show the magnetic field.

Earth

Diploarization seen in the equatorial plane

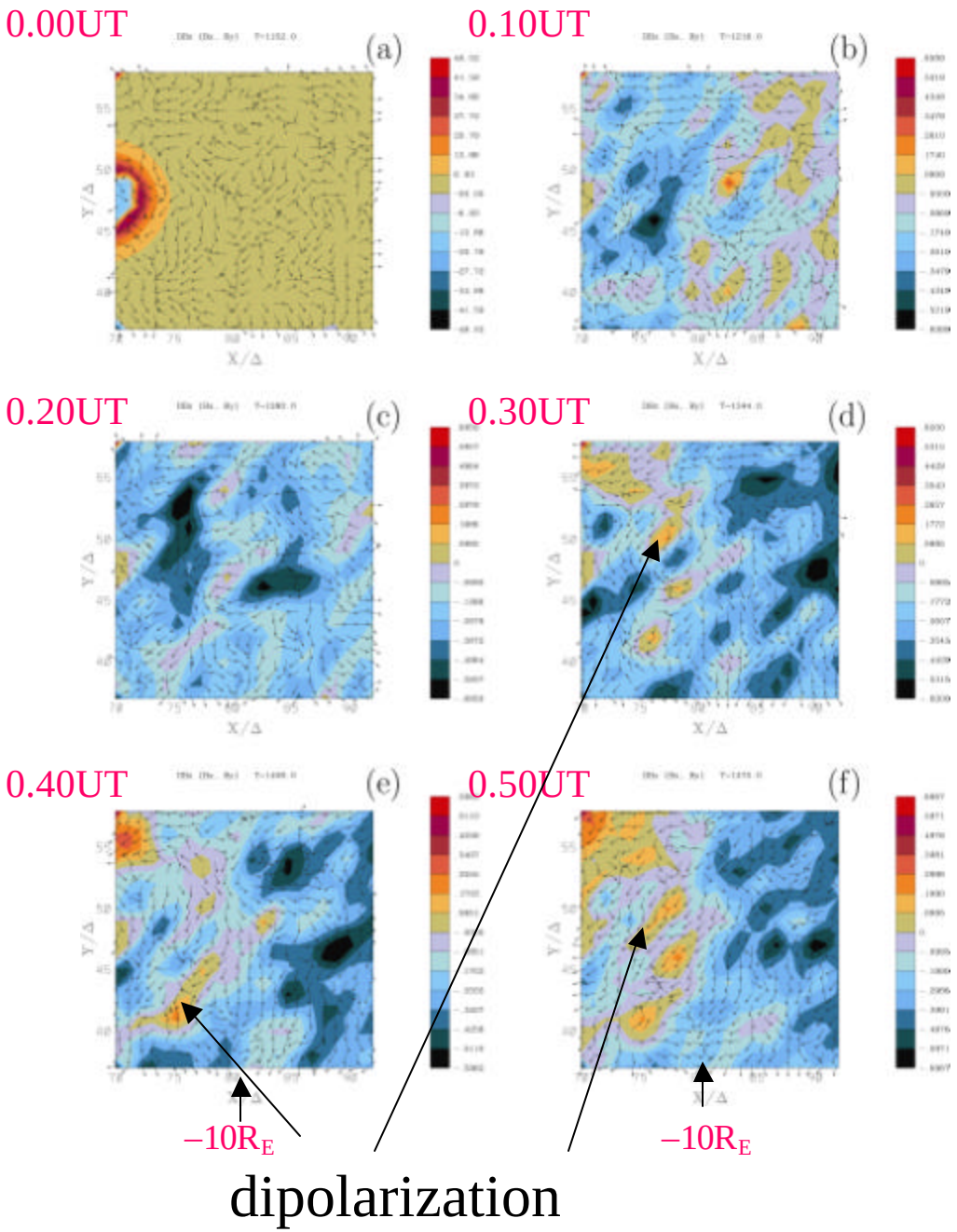

reds: increased

blues: decreased

arrows (B_x, B_y)

Figure 8 shows time evolution of the ***B_z magnetic field component*** subtracted by the value at time 0.00 UT (1152) (a) in the equatorial (x - y) plane near the Earth magnetosphere at time (b) 0.10 UT (1216), (c) 0.20 UT (1280), (d) 0.30 UT (1344), (e) 0.40 UT (1408), and (f) 0.50 UT (1472). The arrows show the magnetic field in the equatorial plane.

Earth

Particle injection at the equatorial plane

Electron density

Arrows: flux

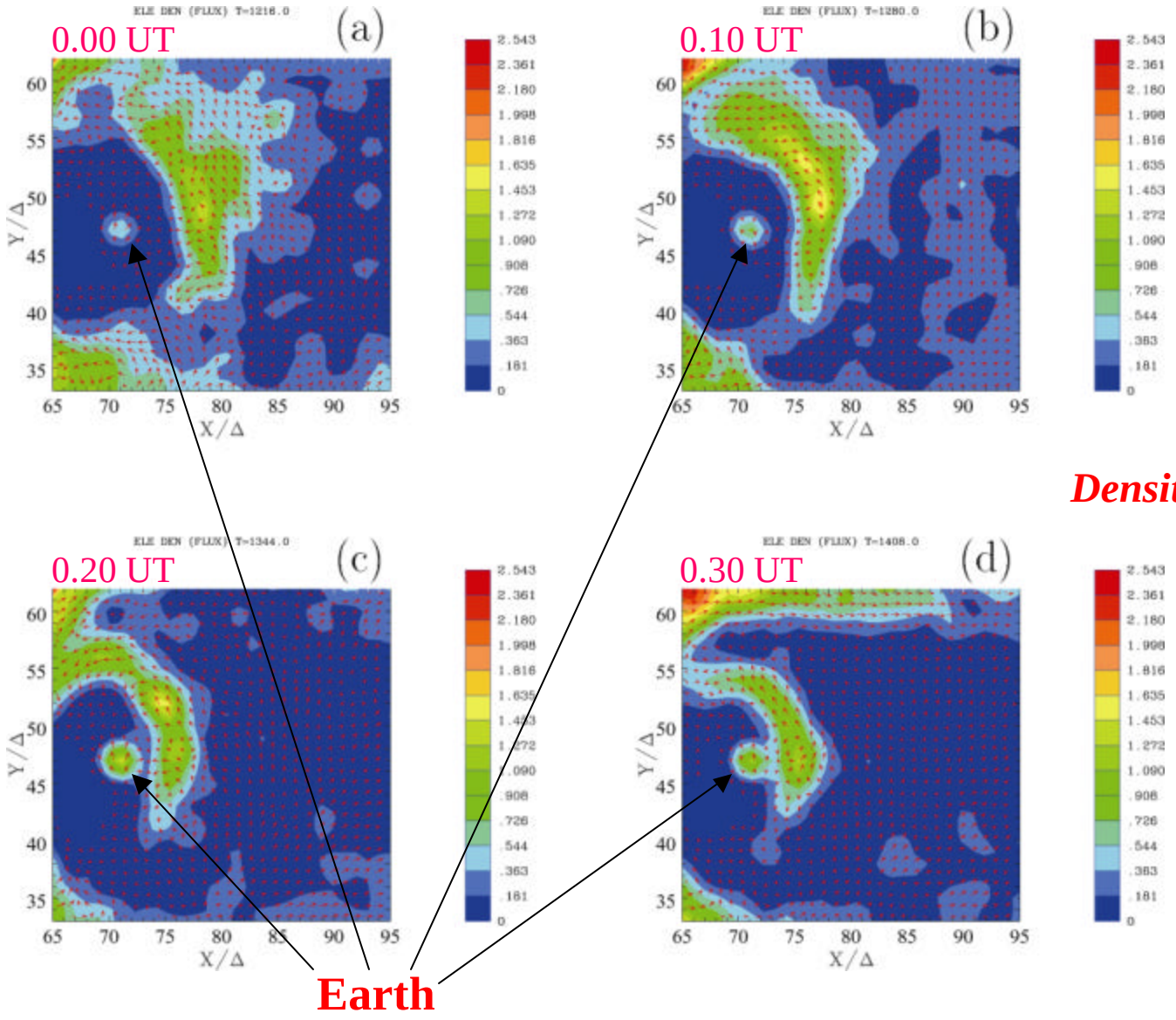

Density: normalized

Field-aligned currents at the north pole at $r = 5\ R_E$

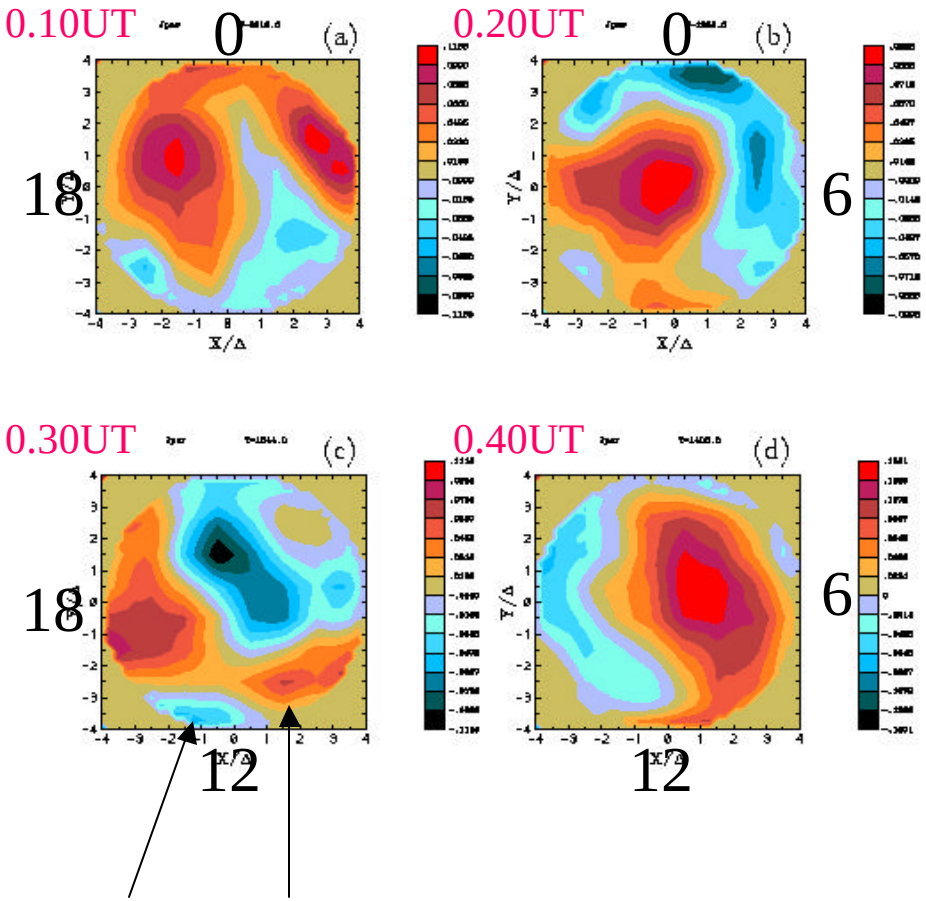

region 2
(wedge current?)

latitudes: 37°- 90°

blues: inward

reds: outward

Figure 9 shows time evolution of the field aligned current at $r = 5\Delta$ ($\approx 5\ R_E$)) around the north pole (90° -- 36.9°) (projected on the equatorial plane and viewed from the pole). (a) 0.10 UT (1216), (b) 0.20 UT (1280), (c) 0.30 UT (1344), and (d) 0.40 UT (1408). The inward and outward currents are shown by blues and reds, respectively.

needs further improvements!

Summary

- Simulation with a southward IMF shows the sequence of substorm processes, which is similar to the observations
- Due to the local reconnection and the convection electric field ($E \approx -V_{sol} \times B_{IMF}$), earthward flows enhance the sheet current at the near the Earth, which leads to current disruption
- Substorm (a wedge current) is triggered by the synergetic effects of reconnection, CD, flow braking, and dipolarization
- In order to investigate the substorm and storm dynamics, a new simulation with better resolutions and a more realistic ionospheric model is required and in progress
- Global particle simulation will be a vital model for Space Weather Program and future investigations with multi-satellite missions such as MMS and MC DRACO

Future Plans

- **Run simulations with better resolutions using HPF Tristan code on ORIGIN2000 with collaboration**
- **Implement a better ionospheric model including ionospheric outflows**
- **Simulations related to magnetic storms including magnetic plasma clouds and investigate and predict high energy particle injections into the ionosphere**
- **Using satellite date for initial solar wind conditions, perform case studies to compare with observations (case studies)**
- **Improve 3-D displays in order to understand physics involved with Tecplot, AVS with virtual satellites**
- **Investigate the dayside magnetopause including Cluster and Interball observations**
- **Global particle simulations will be improved and performed in assistance with multi-satellite missions (MMS, MC DRACO)**